ORIGINAL PAPER

Spatial variations in xylem sap flux density in evergreen oak trees with radial-porous wood: comparisons with anatomical observations

**Makiko Tateishi · Tomo'omi Kumagai · Yasuhiro Utsumi · Toshihiro Umebayashi ·
Yasuki Shiiba · Kazunobu Inoue · Kiyohiro Kaji · Keiichiro Cho · Kyoichi Otsuki**

Abstract To estimate whole-tree water use when employing sap flow measurements, integration of the sap flux density (F_d) over the sapwood area is needed. Accordingly, it is necessary to obtain information on the characteristics of stem water transportation such as spatial variations in F_d and the active xylem area in the stem cross-section. Although evergreen oak trees with radial-porous wood represent a major component of secondary forests in western Japan, detailed information on their stem water transportation characteristics remains unclear. In the present study, we used the heat dissipation method (Granier method) to conduct measurements of azimuthal and radial variations in the F_d of *Quercus glauca* Thunb. ex Murray, a representative evergreen broad-leaved tree in western Japan. Further, by analyzing the anatomy of the xylem structure, we examined why F_d varies spatially in the stem cross-section. By using a dye solution injected into a radial hole bored into the tree trunk, we confirmed that the entire stem is hydroactive. We also compared the spatial variations in F_d and water conductivity per xylem area (K_s) which were estimated by using the observed vessel diameters and their density over the stem cross-section and Hagen–Poiseuille's law. Azimuthal and radial variations in F_d reached about 60 and 50% of the maximum values, respectively, and could be explained by spatial variation in K_s. As a result, we obtained statistical parameters describing the spatial variation in F_d in *Q. glauca* and determined that whole-tree water use estimated from measurements in one direction had at most ±20% potential errors for studied trees.

Keywords Hagen–Poiseuille's law · *Quercus glauca* · Transpiration · Water use · Wood characteristics

Introduction

Evergreen oaks are widely distributed from Southeast Asia to Japan, and are among the most important components of Asian monsoon forests (Hotta 1974). Furthermore, they are a major component of secondary forests in western Japan, and thus play a significant role in water and material cycling in forest ecosystems in this region.

The sap flow technique is the most promising means for obtaining information on forest water cycling in Japan, where most forested areas are situated in mountain regions (Kumagai et al. 2005a, b, 2007). However, during application of this technique, failure to account for spatial (radial and azimuthal) variations in xylem hydraulic characteristics may introduce significant errors when scaling-up sap flux density (F_d) measurements to the whole-tree or stand scale (e.g., Phillips et al. 1996; Lu et al. 2000). Therefore, knowledge regarding spatial variations in F_d of Japanese evergreen oaks within the stem caused by xylem features is of great relevance.

M. Tateishi (✉) · Y. Shiiba · K. Inoue · K. Kaji · K. Cho ·
K. Otsuki
Kasuya Research Forest, Kyushu University,
Sasaguri, Fukuoka 811-2415, Japan
e-mail: tmakiko@forest.kyushu-u.ac.jp

T. Kumagai · Y. Utsumi
Shiiba Research Forest, Kyushu University,
Shiiba-son, Miyazaki 883-0402, Japan

T. Umebayashi
Graduate School of Bioresource
and Bioenvironmental Sciences, Kyushu University,
Hakozaki, Fukuoka 812-8581, Japan

Evergreen oak species (*Lithocarpus*, *Castanopsis*, and *Quercus*) in Japan are clearly characterized by their radial-porous wood anatomy, which is composed of radially oriented files of vessels and well-developed ray tissues (aggregate rays) located in between the files (Wheeler et al. 1989; Itoh 1995). Most deciduous *Quercus* species, on the other hand, have ring-porous wood (e.g., Čermák et al. 1992; Granier et al. 1994; Phillips et al. 1996; Villar-Salvador et al. 1997). To the best of our knowledge, only one study has evaluated the xylem hydraulic characteristics and resulting spatial variation in F_d of Japanese evergreen oak stem (Hirose et al. 2005). Hirose et al. (2005) conducted measurements of sap flow in a 22-year-old *Lithocarpus edulis* (Mak.) Nakai tree, and reported that almost all the stem xylem transported water with large spatial variation in F_d. However, they were only able to relate the radial variation in F_d to the distribution of vessel lumen diameters in a stem cross-section.

Application of sap flow measurements, especially for radial-porous woods, needs to take into account the significant azimuthal variation in F_d resulting from the development of aggregate rays in the stem cross-section. The goal of this study, therefore, is to examine both the radial and azimuthal variations in F_d in stems of Japanese evergreen oak trees and provide appropriate strategies for conducting F_d measurements. Toward this goal, we conducted F_d measurements at several depths and directions in tree trunks of *Quercus glauca* Thunb. ex Murray, a representative evergreen broad-leaved tree in southwestern Japan, and analyzed their xylem structure to explain why F_d spatially varies in the stem.

Materials and methods

Study site and meteorological measurements

The experiments were carried out in two evergreen oak stands in the Kasuya Research Forest, Kyushu University (33°38′N, 130°31′E). The study site, situated in the northern part of Kyushu Island at ∼50 m above sea level, has a mean annual temperature of 16°C and a mean annual precipitation of 1,800 mm.

The stand used for F_d measurements was a botanical garden planted mainly with evergreen oak trees. The majority of the trees are isolated and the grass on the stand floor is cleared a few times during the summer. Micrometeorological conditions were also measured at a large gap in the garden using a solar radiometer (LI-200, Li-Cor, Lincoln, NE, USA) and a temperature and relative humidity sensor (HMP45A, Vaisala, Helsinki, Finland) installed at a height of 1.5 m. Samples were taken every 30 s and averaged over a 30-min period (CR10X,

Campbell Scientific, Logan, UT, USA). At a separate stand located some 500 m south from the stand used for F_d measurements, anatomical observations were conducted using a dye solution injected into the tree trunk.

Sap flow measurements

Flux density measurements were made using the thermal dissipation method with Granier-type sensors (Granier 1987). Each sensor consists of a pair of thermocouple probes 20 mm long and 2 mm in diameter, one of which is inserted into the trunk ∼0.15 m above the other. The upper probe constantly receives 0.2 W of power and heats the sapwood, while the lower one represents the sapwood temperature. The heat is dissipated into the sapwood and vertical sap flux surrounding the probe. The temperature difference between the two probes is then measured and converted into F_d according to Granier (1987). Sap flow signals were scanned every 10 s and 30 min means were recorded on data loggers (CR10X, Campbell Scientific) with multiplexers (AM16/32, Campbell Scientific).

For F_d measurements, we selected four 20-year-old *Q. glauca* trees with a diameter at breast height (DBH) ranging from 0.10 to 0.16 m (Table 1). To investigate the radial and azimuthal variations in F_d, four or five sensors were inserted into each selected tree at several depths and directions as shown in Table 1. First, the 0–20 mm sensors were placed on the given directions around each tree, and then the other depth sensors were placed about 5-cm apart vertically and circumferentially at proximate sensors, at 0.8–1.3 m height. The part of the trunk where the sensors were inserted was fully insulated from the ground to avoid "morning peaks" caused by direct radiation and thermal gradients along the trunk (see Lu et al. 2004). There were few natural thermal gradients along the trunk, and therefore the data did not have to be corrected accordingly.

Table 1 Characteristics of the four *Quercus glauca* Thunb. ex Murray trees studied, and the number and positions of sensors

Tree number	Diameter (m)	Height (m)	Projected crown area (m²)	Directions and depths measured (mm)
393	0.156	6.55	11.89	N 0–20, N 20–40, N 40–60, E 0–20
413	0.113	4.91	2.89	N 0–20, N 20–40, SE 0–20, SW 0–20
414	0.109	4.54	5.81	N 0–20, N 20–40, S 0–20, E 0–20, W 0–20
415	0.098	5.42	5.50	N 0–20, N 20–40, S 0–20, S 20–40

Sap flux density was measured on the *N* north, *E* east, *SE* southeast, *S* south, *SW* southwest, and *W* west directions

The study period for F_d measurements was considered between September 22 and November 30, 2005, because of the ideal environmental conditions at this time; appreciable day-to-day variations in radiation, temperature, and humidity with moist soil conditions. F_d measured during rain events were discarded.

Anatomical observations

Four *Q. glauca* trees with DBH and ages ranging from 0.13 to 0.18 m and 30–39 years, respectively, were used for anatomical observations (Table 2). To visualize water conduction pathways in living trees, we introduced an aqueous solution of 0.2% acid fuchsin into the stems of the study trees (see Sano et al. 2005). Receivers made from plastic funnels were fitted to the stems with vinyl tape and calking compound at a 1 m height above the ground then filled with water. At around noon on September 21, 2005, a hole (12 mm in diameter) was drilled underwater in each receiver to the depth of the pith and the water was then replaced with dye solution. The dye solution was kept in the receivers for 30 min to allow it to flow from the hole into the xylem.

After introduction of the dye solution, we cut down the trees and collected discs at heights of 0, 0.1, 0.3, 0.5 m, and then every 0.5 m above the inlet of the dye solution. Dyed segments in the discs were stored in liquid nitrogen and taken to the laboratory for analysis. After freeze-drying the segments for dye stabilization (see Sano et al. 2005), we counted the number of dyed annual rings from the cambium to the pith with a stereomicroscope (SMZ800, Nikon, Tokyo, Japan).

Furthermore, three radial stem sections were collected from each disc at a height of 1.1 m above the ground to evaluate the effects of vessel characteristics on the spatial variations in F_d. The radial stem sections were rectangular in shape and represented the cambium to the pith in a cross-section of the stem (5 mm circumferential width). Each radial stem section was divided into segments at intervals of 10 mm. The segments were then cut into 10-μm thick cross-sections on a sliding microtome, and stained with

0.1% safranin solution to make the tissues clearly visible. Images of the sections were recorded with a digital camera (Coolpix950, Nikon) through a light microscope (E600, Nikon). We observed the number and diameter of vessel lumina within a 6×3 mm^2 plot in each section by scaling prints from the digital images. The geometric means of the lengths of major and minor axes of single vessel lumina were used as representative values.

Data analysis

The whole-tree sap flow (Q; m^3 m^{-2} s^{-1}) was calculated as the sum of the product of the sap flux ($F_{d20\ i}$) and the cross-sectional area in the direction of each sensor at a given depth (0–20 mm), i:

$$Q = \frac{1}{n}\sum_{i=1}^{n} 0.02\pi(\mathrm{DBH} - 0.02)F_{d20i} + 0.02\pi(\mathrm{DBH} - 0.06)F_{d40i}, \tag{1}$$

where n is the number of directions measured in the xylem at 0–20 mm and $F_{d40\ i}$ is the F_d measured at 20–40 mm. Due to the small area and F_d value at xylem band 40–60 mm of the trees examined (nos. 413 and 414), the sap flow at 40–60 mm was ignored. In addition, we assumed that spatial variation in F_d at depths deeper than the outermost depth could be neglected for Q estimates (e.g., Lu et al. 2000; James et al. 2002; Fernández et al. 2006).

The theoretical water conductivity of a vessel (K_n; kg m MPa^{-1} s^{-1}) was calculated according to Hagen–Poiseuille's law (see Tyree and Zimmermann 2002):

$$K_n = \frac{d^4 \pi \rho}{128\eta_w}, \tag{2}$$

where d is the diameter of a single lumen (m), ρ the density of water at 25°C (kg m^{-3}), and η_W is the viscosity of water (1.0×10^{-9} Mpa s). Note that the K_n of each vessel in a segment was calculated and statistical analysis was applied, i.e., average and standard deviation, for each segment. Furthermore, we considered the theoretical specific conductivity of wood (K_s; kg m^{-1} MPa^{-1} s^{-1}) for the segment, which was calculated by summing all K_n in the segment.

Results and discussion

Spatial variations in F_d observed using the sap flow technique

Figure 1 shows diurnal patterns in the F_d of two given trees (nos. 414 and 393) measured at four directions and three

Table 2 Characteristics of the four *Q. glauca* trees used for anatomical observations

Tree number	Diameter (m)	Height (m)	Age (years)
S1	0.130	11.3	30
S2	0.135	11.8	39
S3	0.140	12.3	37
S4	0.175	14.5	35

depths (see Table 1) under moderate atmospheric evaporative demand. There was considerable azimuthal variation in F_d measured around noon, with the lowest peak value being about 65% of the highest value (Fig. 1b). F_d also decreased with an increase in measurement depth (Fig. 1c). While the peak value of F_d at 20–40 mm was about 60% of that at 0–20 mm, there was little difference in F_d between 20–40 and 40–60 mm.

The decrease in F_d was much steeper between depths of 0–20 and 20–40 mm than between 20–40 and 40–60 mm, and even at 40–60 mm F_d was still about 60% of that at 0–20 mm (Fig. 1c). These findings suggested that almost all of the stem xylem in *Q. glauca* conducts water, and therefore, we further investigated the extent to which vessels are hydroactive in the entire stem cross-section. Our experiments using dye solution confirmed this assumption even in the oldest tree in this study (39-year old) (data not shown). Hirose et al. (2005) found that *L. edulis* has vessels that remain functional for more than 20 years, and thus, it might be a common property of evergreen oaks with radial-porous wood that many vessels conduct water.

Figure 2 further compares the F_d at 0–20 mm and at 20–40 mm for trees nos. 413 and 414 using average F_d measurements around noon (1100–1300 LT). A high correlation between F_d at any two depths has been observed in previous studies (Zang et al. 1996; Lu et al. 2000; Delzon et al. 2004). In this study, F_d at 20–40 mm was linearly related to that at 0–20 mm in all studied trees ($R^2 = 0.58$–0.86). The ratio of F_d at 20–40 to 0–20 mm ranged from 49 to 68% in all studied trees in which the regression coefficient was forced through the origin. In addition, F_d at 0–20 mm at a given direction was correlated with the F_d of other directions ($R^2 = 0.77$–0.92), with ratios ranging from 61 to 97% in all studied trees (see Fig. 3 for trees nos. 413 and 414). Similarly large azimuthal variations in F_d were also reported in previous studies (e.g., Lu et al. 2000; James et al. 2002; Fernández et al. 2006). The azimuthal variations are in a comparable range as the radial variations (e.g., Wullschleger and King
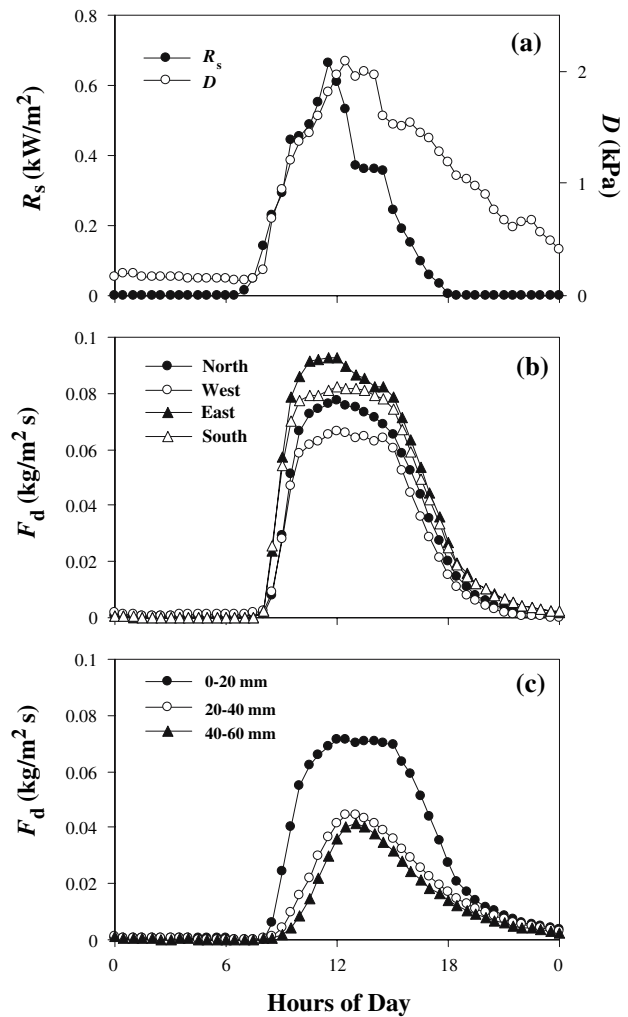

Fig. 1 Diurnal patterns of **a** solar radiation (R_s) and the vapor pressure deficit (D), **b** sap flux density (F_d) at four directions in tree no. 414, and **c** F_d at three depths of sap wood in tree no. 393 on October 3, 2005

2000). This implies that considering the azimuthal variation as well as radial variation in F_d is crucial for estimating whole-tree water use of evergreen oaks.

Fig. 2 Relationship between the F_d at 0–20 mm and that at 20–40 mm for trees nos. 413 and 414, respectively. F_d values represent averaged measurements obtained around noon (1100–1300 LT). Linear regressions were forced through the origin: $y = 0.60\,x$, $R^2 = 0.86$ for tree no. 413, and $y = 0.68\,x$, $R^2 = 0.66$ for tree no. 414
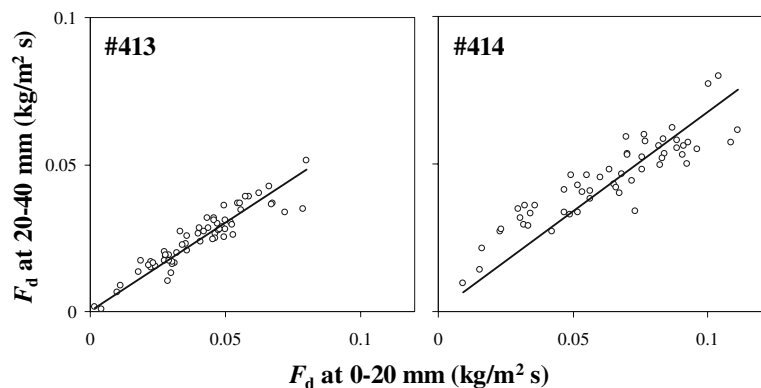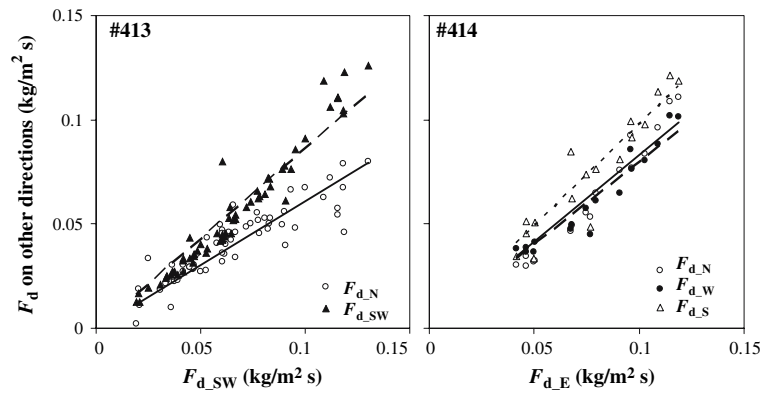
Fig. 3 Relationship between the F_d on a direction and those on other directions. N, E, S, SW, and W denote the directions on which sensors were positioned (north, east, south, southwest, and west, respectively). F_d values represent averaged measurements obtained around noon (1100–1300 LT). Linear regressions were forced through the origin: *solid line*; $y = 0.61\ x$, $R^2 = 0.77$ and *broken line*; $y = 0.86\ x$, $R^2 = 0.92$ for tree no. 413, and *solid line*; $y = 0.83\ x$, $R^2 = 0.91$, *broken line*; $y = 0.80\ x$, $R^2 = 0.92$, and *dotted line*; $y = 0.97\ x$, $R^2 = 0.88$ for tree no. 414

Anatomical explanation for the spatial variation in F_d

While the mean vessel lumen diameter at the outermost depth was around 100 μm and decreased slightly with increasing depth, the vessel density was prone to increasing toward the pith (Fig. 4). The mean lumen diameter in this study was comparable to that in other evergreen *Quercus* species (e.g., Saeki and Harada 1985; Itoh 1995), and its distribution at each depth in the stem cross-sections approximated a Gaussian pattern. Gartner (1995) noted that

Fig. 4 Properties of vessels at 10-mm intervals along the radial direction of a stem cross-section of tree no. S1. Mean lumen diameters (*top*) and vessel densities (*bottom*) are shown. *Vertical bars* represent one standard error

xylem elements declined in density as the cambial age and diameter of the stem increased. The vessel density in this study also decreased with increasing age, partly because density in the radially oriented vessel array decreases toward the bark.

Before discussing the theoretical water conductivity of xylem using the distributions of vessel diameter and density in the stem cross-section (i.e., K_n and K_s), it is necessary to investigate the diameter of functional vessels in water transport. To do so, we first calculated the ratio of the number of dyed vessels of a given diameter class to that of all dyed vessel lumina at each depth in the stem cross-section (P_d). Then, the frequency of a given lumen diameter class (P_x) in their distribution was obtained. According to the ratio P_d/P_x at each depth in all studied trees (nearly constant values against the lumen diameter classes), each diameter class of vessel lumen was equally used in xylem water transport (data not shown). Using soft X-ray photographs of frozen stem sections, Hirose et al. (2005) also reported that most vessel lumina were filled with water in the stem cross-section of an evergreen oak. Therefore, K_n and K_s could sufficiently reflect the properties of xylem water transport in this study.

We suspected that partial cancellations occurred; that is, although a decrease in lumen diameter decreases K_n toward the pith, an increase in vessel density is likely to increase K_s toward the pith (see Fig. 4). Nevertheless, K_n as well as K_s significantly decreased from the outer xylem to pith (Fig. 5), probably because of the larger impact of lumen diameter on the theoretical water conductivity of xylem (see Eq. 2). Thus, we concluded that a reduction in lumen diameter toward the pith primarily contributes to the radial decrease in F_d. Since direct connections between leaves and stem xylem exist only in the outer stem xylem as the leaf longevity of evergreen oaks is 1.7–2.2 years (Kira and
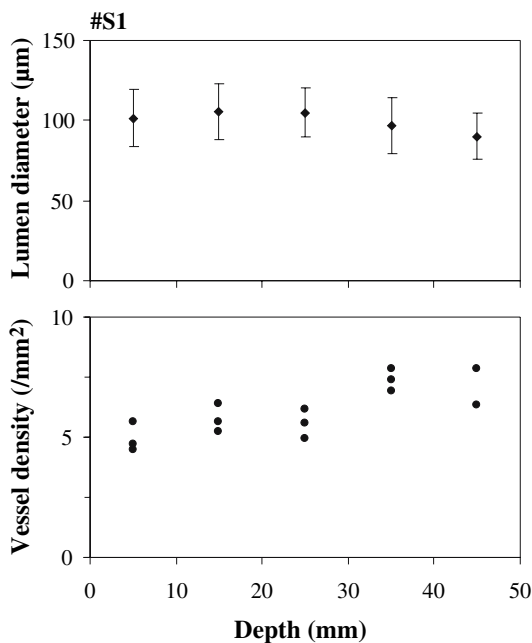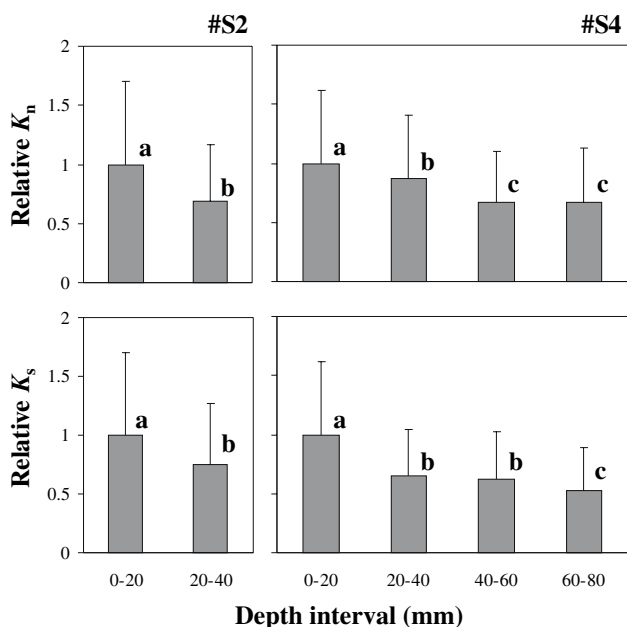
Fig. 5 Ratio of the theoretical water conductivity of a vessel (K_n) at inner depths to that at 0–20 mm (relative K_n) as a function of the depth from the cambium toward the pith in trees nos. S2 and S4 (*top*). As above but with regard to the theoretical specific conductivity of the wood (K_s) (relative K_s; *bottom*). *Vertical bars* represent one standard error. *Bars* with *different letters* are significantly different (Tukey's $P < 0.05$)

Fig. 6 Ratio of the theoretical water conductivity of a vessel (K_n) at directions 2 and 3 to that at direction 1 at 0–20 mm (relative K_n) in trees nos. S1 and S2 (*top*). As above but with regard to the theoretical specific conductivity of the wood (K_s) (relative K_s; *bottom*). *Vertical bars* represent one standard error. *Bars* with *different letters* are significantly different (Tukey's $P < 0.05$)

Yabuki 1978), substantial radial water transport from the inner to outer xylem must occur (see Hirose et al. 2005). Thus, in the studied species, the axial water conductivity of the inner stem xylem might be associated with the abundance of pit pairs in tangential vessel walls and the arrangement and abundance of ray tissue (see Meinzer et al. 2003). Therefore, further investigation with regard to this subject is required.

Both K_n and K_s significantly varied azimuthally, ranging from about 60 to 100% (Fig. 6), which corresponded to the azimuthal variations in F_d in this study (see Fig. 3). Previous studies attributed this fluctuation to the effects of the shaded side of the tree crown (e.g., Oren et al. 1999) and the uneven water distribution in the soil (e.g., Lu et al. 2000). For a radial-porous wood tree, F_d showed significant variation with the different circumferential positions where sap flow sensors were inserted due to its well-developed ray tissue (Hirose et al. 2005). However, we found that the azimuthal variation in vessel lumen diameter in the stem cross-section directly affected the azimuthal variation in F_d.

Whole-tree sap flow calculations

We calculated Q using Eq. 1 for each sample size ($n = 1...3$ and $1...4$ for trees nos. 413 and 414, respectively), over the study period (Fig. 7). The Q-values were expressed as ratios of the values obtained using a given sample size to those obtained using the full sample size. Note that even with a sample size of one, potential errors

Fig. 7 Relationship between sample size and relative whole-tree sap flow in trees nos. 413 and 414. *Sample size* denotes the number of measured directions. *Whole-tree sap flow values* represent averaged measurements obtained around noon (1100–1300 LT) over the study period, and the relative value was obtained as a ratio of the whole-tree sap flow using a given sample size to that using all directions
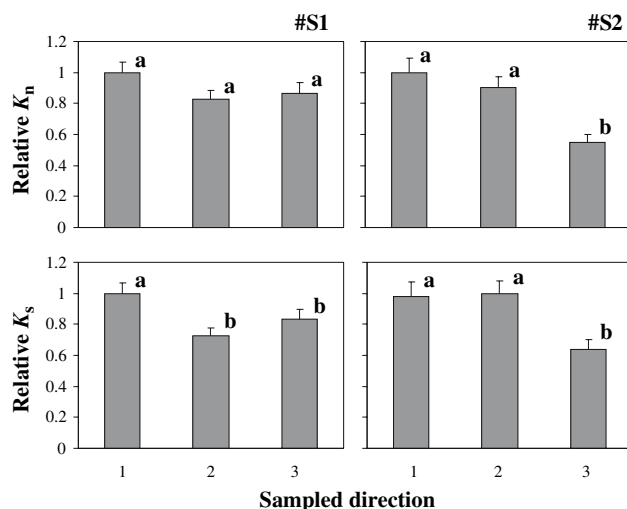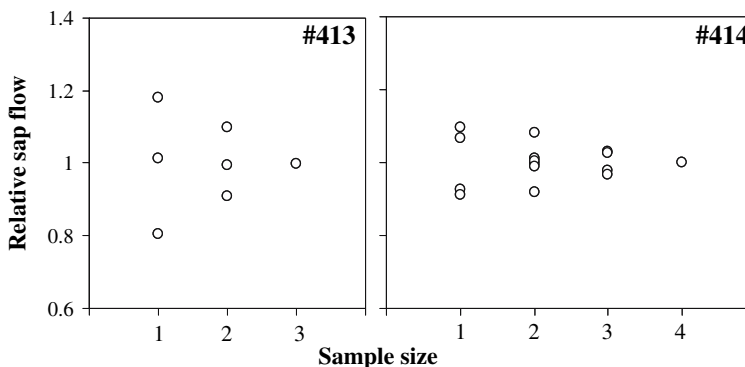
were around ±20 and ±10% for trees nos. 413 and 414, respectively (Fig. 7). The requirement to measure radial variation in F_d when calculating Q was anticipated because it is widely known that failure to take into consideration radial variation introduces a critical error for Q estimates (e.g., Wullschleger and King 2000; Kumagai et al. 2005a).

Azimuthal variations in F_d at the outermost depth have the largest impact on Q estimates, because F_d is generally higher at the outer depth than inner depths and the outermost xylem layers constitute the largest fraction of the total stem cross-section (e.g., Lu et al. 2000; James et al. 2002). In this study, we found that *Q. glauca* trees have an extraordinarily large area of functional xylem. Thus, the relatively higher F_d and their small azimuthal variations due to high vessel density at inner depths might cause a stable Q in the inner xylem area, resulting in stable whole-tree Q estimates (see Fig. 7).

Estimates of water fluxes in forest ecosystems can be obtained by two major approaches: eddy covariance (e.g., Kumagai et al. 2004) and sap flow (e.g., Wullschleger et al. 2001). Eddy covariance typically provides a direct estimate of the water vapor flux released by the forest canopy into the atmosphere. However, this technique has many theoretical limitations, e.g., a flat and homogenous surface is required (e.g., Kaimal and Finnigan 1994). In contrast, the sap flow technique provides information at the single-tree scale and is not limited by complex terrains and spatial heterogeneity. This technique is especially well suited for determining the effects of species composition and other heterogeneous conditions (e.g., Wilson et al. 2001). Despite the robustness of the sap flow technique, scaling procedures are required to extrapolate stand level estimates from sap flux density measurements of individual trees. The information from this study could allow a useful and straightforward treatment of sap flow estimates of transpiration in evergreen *Quercus* trees.

However, it is known that azimuthal and radial variations in F_d change under different soil moisture conditions and atmospheric evaporative demands (e.g., Lu et al. 2000; Nadezhdina et al. 2002). Also, it should be noted that our results were obtained from similar sized or aged individuals of a single evergreen *Quercus* species. Further research is therefore required with regard to the effects of different environmental conditions and age as well as with other Japanese evergreen oak species.

References

Čermák J, Cienciala E, Kučera J, Hallgren JE (1992) Radial velocity profiles of water flow in trunks of *Picea exelsa* and oak and the response of spruce to severing. Tree Physiol 10:367–380

Delzon S, Sartore M, Granier A, Loustau D (2004) Radial profiles of sap flow with increasing tree size in maritime pine. Tree Physiol 24:1285–1293

Fernández JE, Durán PJ, Palomo MJ, Diaz-Espejo A, Chamorro V, Girón IF (2006) Calibration of sap flow estimated by the compensation heat pulse method in olive, plum and orange trees: relationships with xylem anatomy. Tree Physiol 26:719–728

Gartner BL (1995) Patterns of xylem variation within a tree and their hydraulic and mechanical consequences. In: Gartner BL (ed) Plant stems: physiology and functional morphology. Academic, San Diego, pp 125–149

Granier A (1987) Evaluation of transpiration in a Douglas-fir stand by means of sap flow measurements. Tree Physiol 3:309–320

Granier A, Anfodillo T, Sabatti M, Cochard H, Dreyer E, Tomasi M, Valentini R, Bréda N (1994) Axial and radial water flow in the trunks of oak trees: a quantitative and qualitative analysis. Tree Physiol 14:1383–1396

Hirose S, Kume A, Takeuchi S, Utsumi Y, Otsuki K, Ogawa S (2005) Stem water transport of Lithocarpus edulis, an evergreen oak with radial-porous wood. Tree Physiol 25:221–228

Hotta M (1974) History and geography of plants: evolutionary biology in plants, vol 3. Sanseido, Tokyo

Itoh T (1995) Anatomical description of Japanese hardwoods I. Wood Res Tech Notes 31:81–181

James SA, Clearwater MJ, Meinzer FC, Goldstein G (2002) Heat dissipation sensors of variable length for the measurement of sap flow in trees with deep sapwood. Tree Physiol 22:277–283

Kaimal JC, Finnigan JJ (1994) Atmospheric boundary layers flows: their structure and management. Oxford University Press, New York

Kira T, Yabuki K (1978) Primary production rates in the Minamata forest. In: Kira T, Ono Y, Hosokawa T (eds) Biological production in a warm-temperate evergreen oak forest of Japan. Tokyo University Press, Tokyo, pp 131–138

Kumagai T, Aoki S, Nagasawa H, Mabuchi T, Kubota K, Inoue S, Utsumi Y, Otsuki K (2005a) Effects of tree-to-tree and radial variations on sap flow estimates of transpiration in Japanese cedar. Agric For Meteorol 135:110–116

Kumagai T, Aoki S, Shimizu T, Otsuki K (2007) Sap flow estimates of stand transpiration at two slope positions in a Japanese cedar forest watershed. Tree Physiol 27:161–168

Kumagai T, Nagasawa H, Mabuchi T, Ohsaki S, Kubota K, Kogi K, Utsumi Y, Koga S, Otsuki K (2005b) Sources of error in estimating stand transpiration using allometric relationships between stem diameter and sapwood area for *Cryptomeria japonica* and *Chamaecyparis obtusa*. For Ecol Manage 206:191–195

Kumagai T, Saitoh TM, Sato Y, Morooka T, Manfroi OJ, Kuraji K, Suzuki M (2004) Transpiration, canopy conductance and the decoupling coefficient of a lowland mixed dipterocarp forest in Sarawak, Borneo: dry spell effects. J Hydrol 287:237–251

Lu P, Müller WJ, Chacko EK (2000) Spatial variations in xylem sap flux density in the trunk of orchard-grown, mature mango trees under changing soil water conditions. Tree Physiol 20:683–692

Lu P, Urban L, Zhao P (2004) Granier's thermal dissipation probe (TDP) method for measuring sap flow in trees: theory and practice. Acta Bot Sin 46:631–646

Meinzer FC, James SA, Goldstein G, Woodruff D (2003) Whole-tree water transport scales with sapwood capacitance in tropical forest canopy trees. Plant Cell Environ 26:1147–1155

Nadezhdina N, Čermák J, Ceulemans R (2002) Radial patterns of sap flow in woody stems of dominant and understory species: scaling errors associated with positioning of sensors. Tree Physiol 22:907–918

Oren R, Phillips N, Ewers BE, Pataki DE, Megonigal JP (1999) Sap-flux-scaled transpiration responses to light, vapor pressure deficit, and leaf area reduction in a flooded *Taxodium distichum* forest. Tree Physiol 19:337–347

Phillips N, Oren R, Zimmermann R (1996) Radial patterns of xylem sap flow in non-, diffuse- and ring- porous tree species. Plant Cell Environ 19:983–990

Saeki H, Harada H (1985) Cells of hardwood. In: Saeki H, Harada H (eds) Structure of wood. Bun-ei-do, Tokyo, pp 49–100

Sano Y, Okamura Y, Utsumi Y (2005) Visualizing water-conduction pathways of living trees: selection of dyes and tissue preparation methods. Tree Physiol 25:269–275

Tyree MT, Zimmermann MH (2002) Xylem structure and the ascent of sap, 2nd edn. Springer, Berlin

Villar-Salvador P, Castro-Díez P, Pérez-Rontomé C, Montserrt-Martí G (1997) Stem xylem features in three *Quercus* (*Fagaceae*) species along a climatic gradient in NE Spain. Trees 12:90–96

Wheeler EA, Baas P, Gasson PE (1989) IAWA list of microscopic features for hardwood identification. IAWA Bull ns 10:219–332

Wilson KB, Hanson PJ, Mulholland PJ, Baldocchi DD, Wullschleger SD (2001) A comparison of methods for determining forest evapotranspiration and its components: sap-flow, soil water budget, eddy covariance and catchment water balance. Agric For Meteorol 106:153–168

Wullschleger SD, Hanson PJ, Todd DE (2001) Transpiration from a multi-species deciduous forest as estimated by xylem sap flow techniques. For Ecol Manage 143:205–213

Wullschleger SD, King AW (2000) Radial variation in sap velocity as a function of stem diameter and sapwood thickness in a yellow-poplar trees. Tree Physiol 20:511–518

Zang D, Beadle CL, White DA (1996) Variation of sapflow velocity in *Eucalyptus globulus* with position in sapwood and use of a correction coefficient. Tree Physiol 16:697–703